CHEMISTRY OF MATERIALS

pubs.acs.org/cm

Article

Low-Temperature $H_2S/CO_2/CH_4$ Separation in Mixed-Matrix Membranes Containing MFU-4

Qihui Qian,[§] Ashley M. Wright,[§] Hyunhee Lee, Mircea Dincă,* and Zachary P. Smith*

Cite This: https://doi.org/10.1021/acs.chemmater.1c01533

Read Online

ACCESS | Metrics & More | Article Recommendations | Supporting Information

ABSTRACT: Harvesting natural gas and biogas often requires energy-intensive separation processes. Mixed-matrix membranes (MMMs) containing CO_2-selective metal−organic frameworks (MOFs) show great potential in addressing this separation challenge with greater energy efficiency than traditional technologies. Here, we report an MMM system formed from a 6FDA−Durene polymer and an MFU-4 MOF, which demonstrated improved CO_2/CH_4 gas separation performance, especially at low temperatures. Decreasing the temperature from 65 to 15 °C led to a significant increase in CO_2/CH_4 permselectivity for the hybrid MFU-4/6FDA−Durene membrane, with an associated high CO_2 permeability above 1000 barrer. Mixed-gas permeation tests involving H_2S were conducted, and the separation performance of the MFU-4 hybrid membrane was comparable to literature materials specially designed for H_2S separation. For CO_2-based separations, MFU-4 is believed to have a gating effect that favors the linear shape of CO_2. However, a detailed investigation of sorption and diffusion revealed that this specific effect was not clearly accessible under the conditions considered in this study. Instead, the high CO_2/CH_4 permselectivity at low temperature was attributed mainly to the higher polarizability and smaller size of CO_2 compared to CH_4.

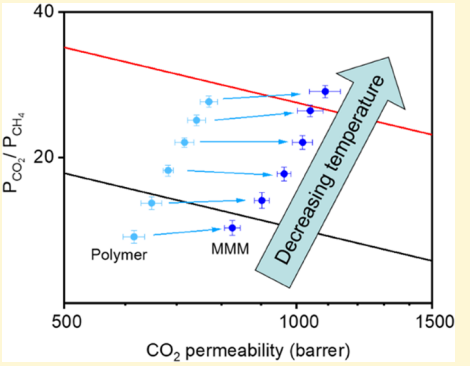

INTRODUCTION

Membrane-based gas separations have many attractive applications, including air separation, hydrogen recovery, natural gas sweetening, and flue gas treatment.[1] Membrane technologies can lower cost, reduce carbon footprint, and simplify operations compared to conventional gas separation technologies.[2,3] However, several challenges need to be overcome to unlock the full potential of membranes. For instance, the primary challenge is the inherent trade-off between gas permeability and permselectivity, as described by the Robeson Upper Bound.[4−8] To overcome this challenge, researchers have focused on creating new membranes with augmented performance by designing new polymers or modifying current polymer systems.[9−11] One of the most promising strategies is to create mixed-matrix membranes (MMMs), which combine a dispersed molecular sieving phase (filler particles) with a continuous polymer phase (matrix).[12] Various dispersed fillers, such as zeolites,[11] carbon molecular sieves,[9] and metal−organic frameworks (MOFs),[12] have been incorporated into polymers to produce MMMs. MOFs are desirable filler materials because their organic linkers often have inherently better compatibility with polymers, or they can be modified to create defect-free films.[1,13,14] In recent years, many researchers have demonstrated that compatible MOF fillers and polymeric matrices can lead to synergistic improvements in both permeability and permselectivity.[15−19] Nevertheless, a key challenge in the field is to identify additional MOF−polymer compositions that simultaneously enhance permeability and permselectivity when compared to pure polymer membranes.

In addition to addressing interfacial compatibility in a specific MMM system, operating conditions (temperature, pressure, etc.) play a critical role in MMM performance.[20] In 2016, Liu and co-workers developed a 6FDA/BPDA−DAM hollow fiber membrane that demonstrated an enhancement in CO_2/N_2 permselectivity at temperatures below 0 °C with negligible CO_2 permeance loss as compared to measurements at ambient temperatures.[20] Later, Liu and co-workers prepared MMMs based on a 6FDA−DAM polyimide and CO_2 affinitive Y-fum-fcu-MOF. Permeation tests conducted at −40 °C revealed an exceptionally high CO_2/CH_4 permselectivity of 130 with an associated CO_2 permeability above 1000 barrer.[21]

Here, we report a MOF−polymer hybrid system for CO_2/CH_4 separation without any chemical or physical alteration to the as-synthesized MOF or polymer materials. We report the performance of an MMM formed from 6FDA−Durene (a widely reported polyimide with high intrinsic separation performance[22]) and an MFU-4 MOF with interconnected

Received: May 3, 2021
Revised: August 9, 2021

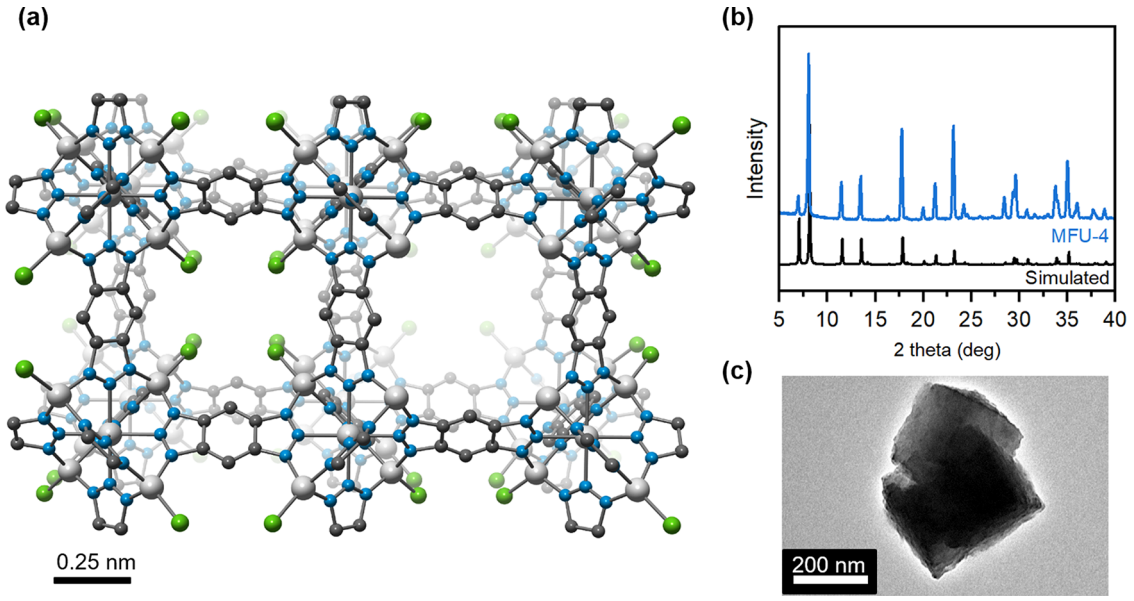

Figure 1. (a) Structure of MFU-4 showing two distinct pore architectures. Chloride atoms on the front right zinc sites in (a) were removed to aid the visualization of the second internal pore. (b) Powder X-ray diffraction pattern of activated MFU-4 compared with the simulated pattern. (c) Scanning electron microscope (SEM) image of the MFU-4 crystallite.

cages of very narrow (2.5 Å) but flexible windows (Figure 1a).[23] Insertion of a low loading (9.4 wt %) of MFU-4 into 6FDA−Durene resulted in improvements in CO_2 permeability without a loss in CO_2/CH_4 permselectivity, surpassing the temperature-adjusted 2008 Robeson Upper Bound.[24] A systematic study at temperatures from 15 to 65 °C was conducted to show that tuning the temperature can further improve membrane performance. MMMs performed well at subambient temperatures, indicating their possible utility at low temperatures.

EXPERIMENTAL SECTION/METHODS

Materials. MFU-4 was synthesized using previously published procedures.[25] The 6FDA−Durene polymer was purchased from Akron Polymers and used as received.

Powder X-ray Diffraction (PXRD). Powder X-ray diffraction (PXRD) patterns were recorded with a Bruker Avance II diffractometer equipped with a $\theta/2\theta$ Bragg−Brentano geometry and Ni-filtered Cu Kα radiation source (Kα_1 = 1.5406 Å, Kα_2 = 1.5444 Å, Kα_1/Kα_2 = 0.5). The tube voltage and current were 40 kV and 40 mA, respectively. Samples for PXRD were prepared by placing the material on a zero-background silicon crystal plate.

Gas Adsorption Isotherms. Gas adsoption isotherms were measured by a volumetric method using a Micromeritics 3Flex gas sorption analyzer. Typical samples of ca. 40−80 mg, preactivated at 150 °C to remove all detectable residual solvents, were transferred to a preweighed analysis tube. The tube with the sample inside was weighed again to determine the mass of the sample. The tube was capped with a Micromeritics TranSeal and transferred to the analysis port of the gas sorption analyzer. Free space correction measurements were performed using ultra-high-purity He gas (UHP grade, 99.999% pure, Airgas). Carbon dioxide and methane isotherms were measured using ultra-high-purity carbon dioxide and methane (99.99%, Airgas). Carbon dioxide and methane analyses were performed at varying temperatures using a water isothermal bath. Oil-free vacuum pumps were used to prevent contamination of sample or feed gases.

Film Casting. Film casting was performed via a solution casting technique. The filler suspension (MFU-4 in chloroform) was mixed with a 6FDA−Durene polymer solution in chloroform to target a casting solution of 2 wt/v % (total solids/suspension volume). Following solvent evaporation, the targeted MMM weight loading of approximately 10 wt % was achieved. To ensure uniform dispersion, suspensions were sonicated directly using a probe sonicator for 1 min and then sonicated indirectly using a water-bath sonicator for 1 h. Suspensions were then stirred for 1 h. This process was repeated three times. Afterward, suspensions were stirred overnight at room temperature before casting. Next, suspensions were poured into flat-bottomed glass Petri dishes and covered by glass plates to prevent contamination from dust and to control the evaporation rate. Solutions were left for 24 h at ambient temperature and pressure to form free-standing films. Films were carefully peeled from the glass dish with the assistance of deionized H_2O. To remove solvent, films were dried in a fume hood for 24 h and then dried under dynamic vacuum in a vacuum oven overnight at 60 °C. Finally, the residual solvent was removed by drying films in a vacuum oven at 150 °C overnight.

Pure-Gas Permeation Tests. Pure-gas permeation tests were performed in an automated, constant-volume/variable-pressure system from Maxwell Robotics to determine the pure-gas permeabilities of He, H_2, O_2, N_2, CH_4, and CO_2. The film areas of approximately 15 mm^2 were cut from the as-prepared films and placed over the top of a small hole on a circular brass supporting disk. The edge of the film was sealed by epoxy glue (Devcon 5 min Epoxy), leaving a small active area of the sample exposed for permeation. The disk was then inserted into a stainless steel permeation cell, sealed, and immersed in a water bath with temperature controlled by an immersion circulator (ThermoFisher SC150L). All gases tested were ultra-high-purity gases purchased from Airgas. Before switching to a new permeating gas, the entire system was dosed with approximately 1 bar of helium and then held under dynamic vacuum for 1 h to ensure no residual gas remained in the tubing. In all cases, the membranes were tested at temperatures from 15 to 65 °C for an upstream pressure of 1 bar. In each case, three films were made and tested to confirm reproducibility. Uncertainties in permeabilities, diffusivities, and solubilities are reported as standard deviations from experiments run in triplicate or by error propagation, as specified for each sample in the Supporting Information (SI).

Mixed-Gas Permeation Tests. Mixed-gas permeation tests were performed using an automated, constant-volume/variable-pressure system from Maxwell Robotics to determine the mixed-gas permeabilities of CH_4, H_2S, and CO_2. An Agilent 7890B GC system was used to analyze the gas composition of both feed and permeant streams. The same membrane coupon and support as that used in

https://doi.org/10.1021/acs.chemmater.1c01533
Chem. Mater. XXXX, XXX, XXX−XXX

pure-gas permeation tests was inserted into a sealed stainless steel permeation cell and temperature was controlled by a built-in air-heating system. Equilibrated gas mixtures of 50:50 CO_2/CH_4, 50:50 H_2S/CH_4, or 60:20:20 $CO_2/H_2S/CH_4$ were produced upstream of the permeation cell using an on-the-fly gas dosing system by Maxwell Robotics. In all cases, membranes were tested at 35 °C for a total upstream pressure of 2 bar. During each permeation step, the permeate was collected in the downstream volume until a steady state was achieved, after which the downstream volume was evacuated and allowed to refill to ~13 Torr. At this point, the downstream gas was injected by a vacuum injection system into the gas chromatograph (GC) so that the composition could be obtained.

RESULTS AND DISCUSSION

MOF $Zn_5Cl_4(bbta)_3$ (**MFU-4**, H_2bbta = 1*H*,5*H*-benzo(1,2-*d*), (4,5-*d*′)bistriazole) is a cubic MOF consisting of two different types of interconnected cages (Figure 1a) with a small aperture window of 2.5 Å between each cage. The aperture is created by eight Zn−Cl bonds that occupy one of the cages, but Zn−Cl bonds are flexible. Since the original development of MFU-4 MOF in 2009,[25] this MOF has shown potential in H_2/D_2 sorption[23] and gas-phase redox catalysis.[26,27] In addition to the abovementioned applications, the high crystallinity, well-defined pore size, and a possible gating mechanism[23] also make this MOF a good candidate as a filler in MMMs for gas separation applications.

In this work, highly crystalline MFU-4 nanoparticles (Figure 1b,c) were first synthesized using a recipe reported elsewhere[25] and then added at 9.4 wt % loadings to a compatible polymer, 6FDA−Durene, to form MMMs via a solvent evaporation method. Cross-sectional SEM images of the MMM are presented in Figure S1, and details on calculating MOF loading from thermogravimetric analysis (TGA) are provided in the SI in the text surrounding Figure S2a. The MMM thickness was 85 ± 2 μm. Figure S2b provides further confirmation of successful insertion of the MFU-4 MOF into the polymer through Fourier transform infrared (FTIR) analysis. As a control, a pure 6FDA−Durene polyimide with a thickness of 63 ± 1 μm was used for side-by-side characterized experiments with the MMM. After the insertion of MFU-4 particles, the density of the film increased from 1.30 ± 0.05 g/cm^3 for the pure polymer to 1.35 ± 0.07 g/cm^3 for the MMM.

Motivation for this study came from Volkmer and colleagues, who reported outstanding CO_2/N_2 adsorption selectivity for MFU-4 due to an unusual gate-driven adsorption effect for CO_2.[28] Computational studies elucidated that CO_2 could activate the Cl gate to remain open during adsorption, whereas N_2 was unable to cause this effect, owing to its shorter molecular length compared to CO_2. We hypothesized that such a gating mechanism could be extended to other CO_2-based separations for MMMs, such as CO_2/CH_4 separation. This hypothesis is supported by a similar adsorption selectivity between CO_2/CH_4 and CO_2/N_2 at 298 K for the MFU-4 powder, which can be gleaned from the isotherms in Figure S4.

Pure-gas permeation tests for CO_2 and CH_4 (Figure 2) were performed on the MFU-4/6FDA−Durene MMM and pure 6FDA−Durene polymer at 1 bar. At 25 °C, the MMM exhibits a significant increase in the CO_2 permeability (1042 barrer) compared to the native polymer (742 barrer), while the CO_2/CH_4 permselectivity of 23.9 ± 1.8 for the polymer and 25.0 ± 1.6 for the MMM are within the uncertainty of each other. Notably, the MMM has performance near the temperature-adjusted upper bound at 25 °C, making this material a promising candidate for CO_2/CH_4 gas separation.

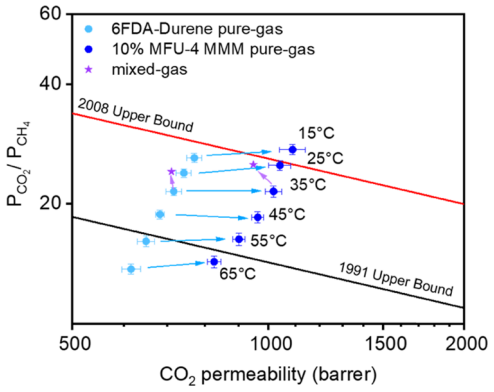

Figure 2. Temperature dependence of gas permeation for 6FDA−Durene and 10% MFU-4 MMM. The 50:50 CO_2/CH_4 mixed-gas experiment was conducted at 2 bar total pressure (purple stars).

To assess membrane performance at various temperatures, we performed pure-gas permeation tests between 15 and 65 °C. Increasing the temperature resulted in lower permselectivity. However, the permselectivity of the MMM consistently showed similar results to that of the native 6FDA−Durene polymer. In contrast, under subambient conditions (15 °C), we observe a significant improvement in permselectivity of the MMM, with a permselectivity of 27.4 and permeability of 1090 barrer.

Because of the predicted gate opening effect for CO_2,[28] we performed a mixed-gas permeation experiment using 50:50 CO_2/CH_4 at 2 bar total pressure and 35 °C (Figure 2). We had anticipated that the gating effect would improve CH_4 permeation while co-permeating with CO_2 because CO_2 would expand the framework pores, but results demonstrated the opposite effect. The mixed-gas permselectivity (25.1) is higher than single gas experiments, although the CO_2 permeability is slightly lower (949 barrer). CH_4 permeability exhibited a more significant decrease between the pure and mixed-gas experiments (from 47.4 to 37.8 barrer), suggesting that a competitive sorption effect[29] has a more significant influence on transport than the gate opening effect under the conditions tested.

For polymeric membranes and MMMs with low loadings, the solution-diffusion model has been widely used to describe the transport of gas molecules in these films.[1] According to the model, permeation, *P*, of a gas through a film depends on two processes: diffusion, *D*, and sorption, *S*. The equation, $P = D \times S$, was used to decouple the gas permeability into effective diffusion and sorption coefficients. To gain further insights into the mechanism of transport, we used the time-lag method to estimate the diffusivity and sorption of CO_2 and CH_4 in the 10 wt % MMM (Figure 3). We also collected data for N_2 and O_2 to expand our analysis to other gases of interest. The diffusion coefficients decreased with decreasing temperatures (Figure 3a), whereas the sorption coefficients increased with decreasing temperatures for all examined gases (Figure 3b). Temperature more significantly influences the sorption of CO_2 than that of the other gases examined, which is a result of the higher polarizability of CO_2 and the more negative activation energy of sorption, which will be discussed later. Consequently, CO_2 exhibits higher sorption coefficients than the other gases, which results in increased sorption selectivity at lower temperatures (Table 1). A similar analysis on the pure

https://doi.org/10.1021/acs.chemmater.1c01533
Chem. Mater. XXXX, XXX, XXX−XXX

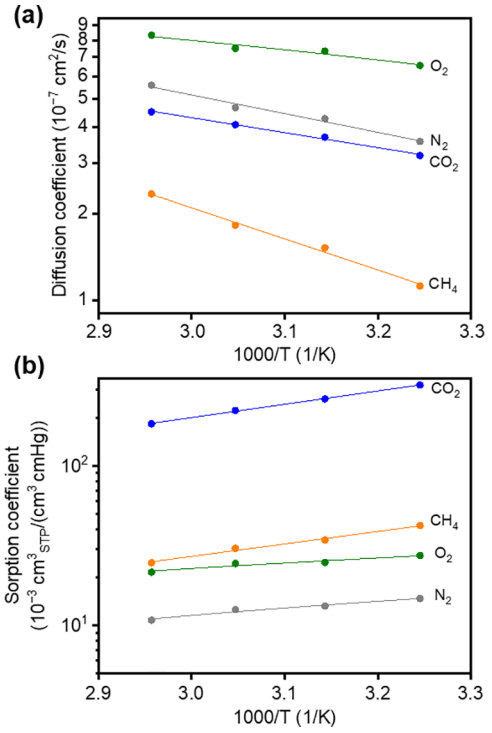

Figure 3. Van't Hoff plots for (a) diffusion and (b) sorption of carbon dioxide, oxygen, nitrogen, and methane in the MMM.

Table 1. Comparison of the Temperature Dependence on CO_2/CH_4 Permselectivity, Diffusion Selectivity, and Sorption Selectivity in the MMM

	CO_2/CH_4 selectivity		
temperature (°C)	permeation	diffusion	sorption
35	21.5	2.8	7.7
45	18.5	2.4	7.5
55	16.3	2.2	7.4
65	14.3	1.9	7.3

polymer film can be found in Figure S3, which shows general trends of lower diffusion and sorption coefficients compared to the MMM at all temperatures, but otherwise, the correlations are similar.

CO_2 permeability increased slightly with decreasing temperatures (Figure 2). This finding results from the competition between increased sorption and decreased diffusion with decreasing temperatures. Notably, even though sorption selectivity contributes more to the high permselectivity of the MMM, a significant increase in diffusion selectivity at a lower temperature is the major cause of the overall performance improvement at lower temperatures (Table 1). We observed a different trend in the case of the pure polymer film (Table S1). Diffusion selectivity remained consistent across different temperatures, whereas an increase in sorption selectivity drove the increase in permselectivity at lower temperatures. This result suggests that MFU-4 plays an important role in altering the diffusion and sorption affinity of the MMM toward CO_2 and CH_4. Next, we calculated the activation energies of diffusion, sorption, and permeation in the MMM to further elucidate temperature effects on transport (Figures 4 and 5). There is an inverse relationship between the activation energy of sorption and the critical temperature (T_c) of the penetrant gas (Figure 4a). This finding is expected when the enthalpy change from the gas phase to the sorbed phase dominates over the enthalpy of mixing, as would be expected for the gases considered here.[30] Likewise, semi-log plots of sorption versus $(T_c/T)^2$ display a linear trend (Figure 4d). On the other hand, the activation energy of diffusion generally increases with the increasing diameter of the gases (Figure 4b) following trends expected from the Brandt model.[31] Table S2 summarizes the diameters of examined gases in this work, and it should be noted that we present diffusion correlation diameters, d_{dc}, derived from upper bound analysis,[4−6] which exhibited the strongest correlation with our data. The energy barrier for diffusion is greater for larger molecules resulting in high diffusion selectivities based on molecular size. Overall, the activation energy of permeation is negative for CO_2 but positive for CH_4 (Figure 4c). Consequently, as temperature decreases, permeation increases for CO_2 but decreases for CH_4, thereby increasing permselectivity.

Compared to control experiments on the pure polymer (Figure S5), there was one notable difference in transport behavior for the MMM. Upon insertion of MFU-4, the activation energy of diffusion developed a strong dependence on penetrant size. Because of this feature, CO_2/CH_4 diffusion selectivity increased by nearly 50% for the MMM as the sample was cooled from 65 to 35 °C, whereas the pure polymer showed almost no difference in size screening over this temperature range. This finding can be visualized by recasting data in the form of Figure 5. Added diffusion selectivity from MFU-4 provides a benefit to permselectivity, but these results are somewhat mitigated by a weakly counteracting sorption effect. Tabulated data for diffusion, sorption, and permeation in the MMM and the pure polymer can be found in Tables S3 and S4.

We compared direct adsorption for CO_2, N_2, and CH_4 in MFU-4 (Figure S4), indicating similar trends to those of Volkmer for CO_2 and N_2.[28] More specifically, Volkmer reported high sorption selectivity of CO_2 over N_2 in MFU-4 due to a CO_2-driven gating effect in the MOF.[28] From their simulations, when CO_2 passes through the framework, it passes through the pores (Figure 1a), which consist of eight Zn−Cl bonds. For a small molecule to pass through the intercage windows, the Zn−Cl bond must distort to open the aperture. In the case of CO_2, its shape forces the Zn−Cl bonds to remain distorted while CO_2 occupies the pore space. To move through the framework, a second Zn−Cl bond that is near a neighboring pore (Figure 1a) also needs to distort. In contrast, due to its shorter and more spherical shape, N_2 passes through the pore and resides there without distorting the Zn−Cl bonds. The overall consequence of inserting MFU-4 into 6FDA−Durene would be an expected enhancement of the CO_2/N_2 diffusion selectivity, and by extension, a possible enhancement of CO_2/CH_4 diffusion selectivity based on the similar adsorption trends between N_2 and CH_4 (Figure S4).

Our transport analysis provides a unique opportunity to evaluate if the CO_2-gating mechanism enhances membrane performance. From Figure 4d,e, it is clear that MFU-4 MMMs follow sorption and diffusion trends that are consistent across all gases. Furthermore, control experiments on the pure polymer (Figure S5) demonstrate standard trends in sorption and diffusion, suggesting that no unique transport effects in MFU-4 are concealed by the polymer phase. A gating mechanism specific to CO_2 would require distinct diffusion behavior for this molecule relative to trends for nongating gas species. Regrettably, these trends were not observed in our

https://doi.org/10.1021/acs.chemmater.1c01533
Chem. Mater. XXXX, XXX, XXX−XXX

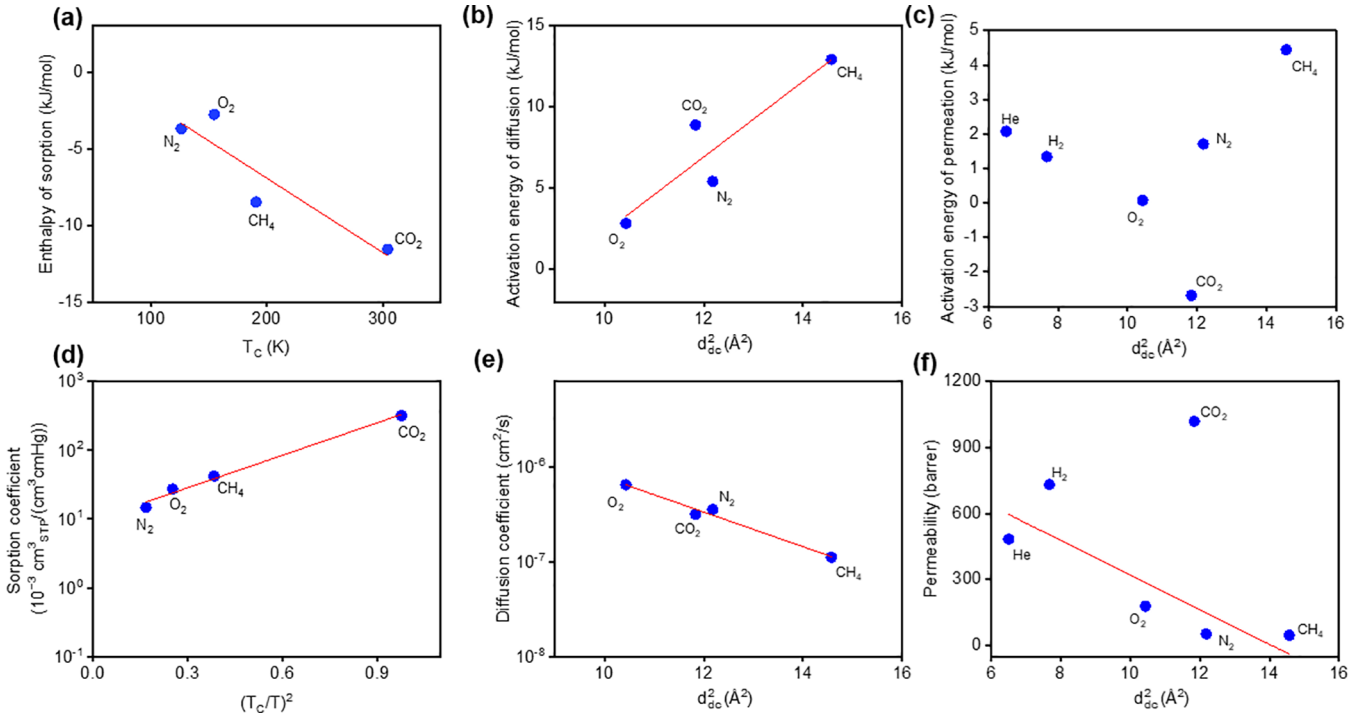

Figure 4. (a–c) Activation enthalpies and (d–f) transport performance trends of sorption, diffusion, and permeation in the MMM. The term d_{dc} is the diffusion correlation diameter.[36,37]

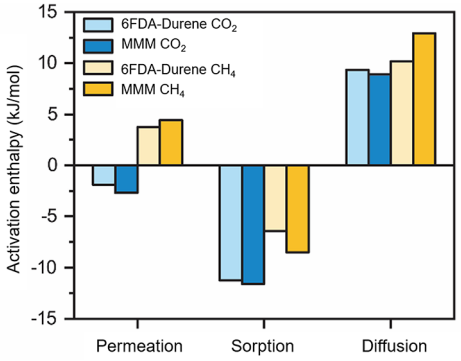

Figure 5. Activation enthalpies for permeation, sorption, and diffusion for CO_2 and CH_4 in 6FDA–Durene and MMM.

experiments, indicating that the effect of gating in MFU-4 is small relative to other modes of transport under the conditions that were considered. Nevertheless, the intrinsic properties of this MOF still demonstrate intriguing separation performance.

Many natural gas and biogas streams contain H_2S, which must be removed to meet pipeline specifications.[32,33] Therefore, we evaluated the MMM using a mixed-gas permeation test with H_2S to probe the potential of MFU-4 MMMs in a more realistic separation environment. For a binary 50:50 H_2S/CH_4 feed stream, H_2S permeability of 384 barrer and H_2S/CH_4 permselectivity of 13.1 were observed at 2 bar total pressure and 35 °C. For a ternary 60:20:20 $CO_2/H_2S/CH_4$ feed at 2 bar total pressure and 35 °C, a lower H_2S permeability (316 barrer) and H_2S/CH_4 permselectivity (11.3) were observed, indicating possible conditioning and plasticization effects in these MMMs. However, the combined $(H_2S + CO_2)/CH_4$ permselectivity reached a remarkable value of 42, comparable to other MMMs embedded with MOFs specially designed for H_2S separation[34,35] (Figure 6 and Table S5). These findings are encouraging for applying MFU-4 MOFs for membrane-based separations of natural gas or biogas.

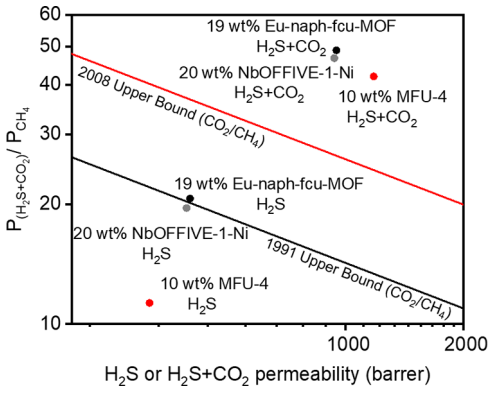

Figure 6. Mixed-gas permeation data of 10% MFU-4 MMM compared to literature materials.

CONCLUSIONS

In conclusion, an MFU-4 MOF was embedded into a 6FDA–Durene polyimide to form a high-performance MMM for natural gas or biogas separation applications. Pure-gas and mixed-gas permeation results show that the 10 wt % MMM exhibited high CO_2 and H_2S permeability with excellent permselectivity. A systematic temperature study for pure-gas permeation was conducted to evaluate the impact of testing temperature. Lowering the temperature led to improved CO_2 permeability and increased CO_2/CH_4 permselectivity, with property sets near the temperature-adjusted 2008 Upper Bound. Improvements in separation performance of the MMM relative to the polymer were mainly due to the higher

https://doi.org/10.1021/acs.chemmater.1c01533
Chem. Mater. XXXX, XXX, XXX–XXX

polarizability and smaller size of CO_2 compared to CH_4, and no significant gating effects were observed within the testing temperatures. The MMM also showed excellent performance at low pressures when tested in the presence of H_2S. This work demonstrates the potential for MFU-4 as a promising MMM filler for natural gas and biogas separations, especially at low temperatures.

■ ASSOCIATED CONTENT

Supporting Information

The Supporting Information is available free of charge at https://pubs.acs.org/doi/10.1021/acs.chemmater.1c01533.

Cross-sectional SEM images for the MMM; MMM loading calculation; TGA and FTIR of the MFU-4 MOF and the MMM; diffusion and sorption coefficient van't Hoff plots in the pure polymer film; sorption isotherms for the pure MOF; comparison of the temperature dependence of transport selectivities in the pure polymer film; diffusion correlation diameters of common gas molecules; activation enthalpies and transport performance trends in the pure polymer film; tabulated transport data for the MMM and the pure polymer film with uncertainties; and mixed-gas permeation data of literature materials (PDF)

■ AUTHOR INFORMATION

Corresponding Authors

Mircea Dincă − *Department of Chemistry, Massachusetts Institute of Technology, Cambridge, Massachusetts 02139, United States;* orcid.org/0000-0002-1262-1264; Email: mdinca@mit.edu

Zachary P. Smith − *Department of Chemical Engineering, Massachusetts Institute of Technology, Cambridge, Massachusetts 02139, United States;* orcid.org/0000-0002-9630-5890; Email: zpsmith@mit.edu

Authors

Qihui Qian − *Department of Chemical Engineering, Massachusetts Institute of Technology, Cambridge, Massachusetts 02139, United States;* orcid.org/0000-0002-4057-9315

Ashley M. Wright − *Department of Chemistry, Massachusetts Institute of Technology, Cambridge, Massachusetts 02139, United States;* orcid.org/0000-0002-9475-2638

Hyunhee Lee − *Department of Chemical Engineering, Massachusetts Institute of Technology, Cambridge, Massachusetts 02139, United States*

Complete contact information is available at: https://pubs.acs.org/10.1021/acs.chemmater.1c01533

Author Contributions

[§]Q.Q. and A.M.W contributed equally to this work.

Notes

The authors declare no competing financial interest.

■ ACKNOWLEDGMENTS

The authors gratefully acknowledge support for this study from the MIT Tata Center for Technology and Design.

■ REFERENCES

(1) Qian, Q.; Asinger, P. A.; Lee, M. J.; Han, G.; Mizrahi Rodriguez, K.; Lin, S.; Benedetti, F. M.; Wu, A. X.; Chi, W. S.; Smith, Z. P. MOF-Based membranes for Gas Separations. *Chem. Rev.* **2020**, *120*, 8161−8266.

(2) Zornoza, B.; Tellez, C.; Coronas, J.; Gascon, J.; Kapteijn, F. Metal-Organic Framework Based Mixed Matrix Membranes: An Increasingly Important Field of Research with a Large Application Potential. *Microporous Mesoporous Mater.* **2013**, *166*, 67−78.

(3) Koros, W. J.; Zhang, C. Materials for Next-Generation Molecularly Selective Synthetic Membranes. *Nat. Mater.* **2017**, *16*, 289−297.

(4) Robeson, L. M. Correlation of Separation Factor versus Permeability for Polymeric Membranes. *J. Membr. Sci.* **1991**, *62*, 165−185.

(5) Freeman, B. D. Basis of Permeability/Selectivity Tradeoff Relations in Polymeric Gas Separation Membranes. *Macromolecules* **1999**, *32*, 375−380.

(6) Robeson, L. M. The Upper Bound Revisited. *J. Membr. Sci.* **2008**, *320*, 390−400.

(7) Lin, H.; Yavari, M. Upper Bound of Polymeric Membranes for Mixed-gas CO_2/CH_4 Separations. *J. Membr. Sci.* **2015**, *475*, 101−109.

(8) Burns, R. L.; Koros, W. J. Defining the Challenges for C_3H_6/C_3H_8 Separation Using Polymeric Membranes. *J. Membr. Sci.* **2003**, *211*, 299−309.

(9) Rungta, M.; Xu, L.; Koros, W. J. Carbon Molecular Sieve Dense Film Membranes Derived from Matrimid for Ethylene/Ethane Separation. *Carbon* **2012**, *50*, 1488−1502.

(10) Wu, A. X.; Drayton, J. A.; Smith, Z. P. The Perfluoropolymer Upper Bound. *AlChE J.* **2019**, *65*, 1−12.

(11) Dechnik, J.; Gascon, J.; Doonan, C. J.; Janiak, C.; Sumby, C. J. Mixed-Matrix Membranes. *Angew. Chem., Int. Ed.* **2017**, *56*, 9292−9310.

(12) Seoane, B.; Coronas, J.; Gascon, I.; Benavides, M. E.; Garvan, O.; Caro, J.; Kapteijn, F.; Gascon, J. Metal-Organic Framework Based Mixed Matrix Membranes: A Solution for Highly Efficient CO_2 Capture. *Chem. Soc. Rev.* **2015**, *44*, 2421−2454.

(13) Sun, Y.; Zhou, H. C. Recent Progress in the Synthesis of Metal-Organic Frameworks. *Sci. Technol. Adv. Mater.* **2015**, *16*, No. 054202.

(14) Sabetghadam, A.; Seoane, B.; Keskin, D.; Duim, N.; Rodenas, T.; Shahid, S.; Sorribas, S.; Guillouzer, C.; Le; Clet, G.; Tellez, C.; et al. Metal-Organic Framework Crystals in Mixed-Matrix Membranes: Impact of the Filler Morphology on the Gas Separation Performance. *Adv. Funct. Mater.* **2016**, *26*, 3154−3163.

(15) Yang, T.; Chung, T. S. Room-Temperature Synthesis of ZIF-90 Nanocrystals and the Derived Nano-Composite Membranes for Hydrogen Separation. *J. Mater. Chem. A.* **2013**, *1*, 6081−6090.

(16) Waqas Anjum, M.; Bueken, B.; De Vos, D.; Vankelecom, I. F. J. MIL-25(Ti) Based Mixed Matrix Membranes for CO_2 Separation from CH_4 and N_2. *J. Membr. Sci.* **2016**, *502*, 21−28.

(17) Nik, O. G.; Chen, X. Y.; Kaliaguine, S. Functionalized Metal Organic Framework-Polyimide Mixed Matrix Membranes for CO_2/CH_4 Separation. *J. Membr. Sci.* **2012**, *413*−*414*, 48−61.

(18) Anjum, M. W.; Vermoortele, F.; Khan, A. L.; Bueken, B.; De Vos, D. E.; Vankelecom, I. F. J. Modulated UiO-66-Based Mixed-Matrix Membranes for CO_2 Separation. *ACS Appl. Mater. Interfaces* **2015**, *7*, 25193−25201.

(19) Wang, Z.; Yuan, J.; Li, R.; Zhu, H.; Duan, J.; Guo, Y.; Liu, G.; Jin, W. ZIF-301 MOF/6FDA-DAM Polyimide Mixed-Matrix Membranes for CO_2/CH_4 Separation. *Sep. Purif. Technol.* **2021**, *264*, No. 118431.

(20) Zhang, C.; Dai, Y.; Johnson, J. R.; Karvan, O.; Koros, W. J. High Performance ZIF-8/6FDA-DAM Mixed Matrix Membrane for Propylene/Propane Separations. *J. Membr. Sci.* **2012**, *389*, 34−42.

(21) Liu, L.; Qiu, W.; Sanders, E. S.; Ma, C.; Koros, W. J. Post-combustion Carbon Dioxide Capture via 6FDA/BPDA-DAM Hollow Fiber Membranes at Sub-ambient Temperatures. *J. Membr. Sci.* **2016**, *510*, 447−454.

(22) Liu, Y.; Liu, G.; Zhang, C.; Qiu, W.; Yi, S.; Chernikova, V.; Chen, Z.; Belmabkhout, Y.; Shekhah, O.; Eddaoudi, M.; Koros, W. J. Enhanced CO_2/CH_4 Separation Performance of a Mixed Matrix

Membrane Based on Tailored MOF-Polymer Formulations. *Adv. Sci.* **2018**, *5*, No. 1800982.
(23) Lin, W. H.; Chung, T. S. Gas Permeability, Diffusivity, Solubility, and Aging Characteristics of 6FDA-durene Polyimide Membranes. *J. Membr. Sci.* **2001**, *186*, 183−193.
(24) Teufel, J.; Oh, H.; Hirscher, M.; Wahiduzzaman, M.; Zhechkov, L.; Kuc, A.; Heine, T.; Denysenko, D.; Volkmer, D. MFU-4 − A Metal-Organic Framework for Highly Effective H_2/D_2 Separation. *Adv. Mater.* **2013**, *25*, 635−639.
(25) Rowe, B. W.; Robeson, L. M.; Freeman, B. D.; Paul, D. R. Influence of Temperature on the Upper Bound: Theoretical Considerations and Comparison with Experimental Results. *J. Membr. Sci.* **2010**, *360*, 58−69.
(26) Biswas, S.; Grzywa, M.; Nayek, H. P.; Dehnen, S.; Senkovska, I.; Kaskel, S.; Volkmer, D. A cubic Coordination Framework Constructed from Benzobistriazolate Ligands and Zinc Ions Having Selective Gas Sorption Properties. *Dalton Trans.* **2009**, *33*, 6487−6495.
(27) Denysenko, D.; Wener, T.; Grzywa, M.; Puls, A.; Hagen, V.; Eickerling, G.; Jelic, J.; Reuter, K.; Volkmer, D. Reversible Gas-phase Redox Processes Catalyzed by Co-exchanged MFU-4l. *Chem. Commun.* **2012**, *48*, 1236−1238.
(28) Dubey, R. J. C.; Comito, R. J.; Wu, Z.; Zhang, G.; Rieth, A. J.; Hendon, C. H.; Miller, J. T.; Dinca, M. Highly Stereoselective Heterogeneous Diene Polymerization by Co-MFU-4l: A Single-Site Catalyst Prepared by Cation Exchange. *J. Am. Chem. Soc.* **2017**, *139*, 12664−12669.
(29) Sastre, G.; Bergh, J.; Kapteijn, F.; Denysenko, D.; Volkmer, D. Unveiling the Mechanism of Selective Gate-Driven Diffusion of CO_2 over N_2 in MFU-4 Metal-Organic Framework. *Dalton Trans.* **2014**, *43*, 9612−9619.
(30) Ricci, E.; Benedetti, F. M.; Dose, M. E.; De Angelis, M. G.; Freeman, B. D.; Paul, D. R. Competitive Sorption in CO_2/CH_4 Separations: the Case of HAB-6FDA Polyimide and its TR Derivative and a General Analysis of its Impact on the Selectivity of Glassy Polymers at Multicomponent Conditions. *J. Membr. Sci.* **2020**, *612*, No. 118374.
(31) Matteucci, S.; Yampolskii, Y.; Freeman, B. D.; Pinnau, I. Transport of Gases and Vapors in Glassy and Rubbery Polymers. *Mater. Sci. Membr. Gas Vap. Sep.* **2006**, 1−47.
(32) Brandt, W. W.; Anysas, G. A. Diffusion of Gases in Fluorocarbon Polymers. *J. Appl. Polym. Sci.* **1963**, *7*, 1919−1931.
(33) Baker, R. W.; Lokhandwala, K. Natural Gas Processing with Membranes: an Overview. *Ind. Eng. Chem. Res.* **2008**, *47*, 2109−2121.
(34) Chuah, C. Y.; Goh, K.; Yang, Y.; Gong, H.; Li, W.; Karahan, H. E.; Guiver, M. D.; Wang, R.; Bae, T. H. Harnessing Filler Materials for Enhancing Biogas Separation Membranes. *Chem. Rev.* **2018**, *118*, 8655−8769.
(35) Liu, G.; Cadiau, A.; Liu, Y.; Adil, K.; Chernikova, V.; Carja, I.; Belmabkhout, Y.; Karunakaran, M.; Shekhah, O.; Zhang, C.; Itta, A. K.; Yi, S.; Eddaoudi, M.; Koros, W. J. Enabling Fluorinated MOF-Based Membranes for Simultaneous Removal of H_2S and CO_2 from Natural Gas. *Angew. Chem., Int. Ed.* **2018**, *57*, 14811−14816.
(36) Liu, G.; Chernikova, V.; Liu, Y.; Zhang, K.; Belmabkhout, Y.; Shekhah, O.; Zhang, C.; Yi, S.; Eddaoudi, M.; Koros, W. J. Mixed Matrix Formulations with MOF Molecular Sieving for Key Energy-Intensive Separations. *Nat. Mater.* **2018**, *17*, 283−289.
(37) Robeson, L. M.; Smith, Z. P.; Freeman, B. D.; Paul, D. R. Contributions of Diffusion and Solubility Selectivity to the Upper Bound Analysis for Glassy Gas Separation Membranes. *J. Membr. Sci.* **2014**, *453*, 71−83.

https://doi.org/10.1021/acs.chemmater.1c01533
Chem. Mater. XXXX, XXX, XXX−XXX